



RESEARCH ARTICLE

# A 1179-yr (417–1595 CE) tree-ring oxygen isotope chronology for northern Japan validated using the 774–775 CE radiocarbon spike

Masaki Sano<sup>1</sup> , Zhen Li<sup>2</sup>, Akane Tsushima<sup>3</sup>, Katsuhiko Kimura<sup>4</sup>, Toshio Nakamura<sup>5</sup>, Motonari Ohyama<sup>6</sup>, Minoru Sakamoto<sup>1</sup> , Takeshi Nakatsuka<sup>2</sup> and Masataka Hakozaiki<sup>1</sup>

<sup>1</sup>National Museum of Japanese History, Sakura, Japan, <sup>2</sup>Graduate School of Environmental Studies, Nagoya University, Nagoya, Japan, <sup>3</sup>Graduate School of Science, Chiba University, Chiba, Japan, <sup>4</sup>Faculty of Symbiotic Systems Science, Fukushima University, Fukushima, Japan, <sup>5</sup>Institute for Space-Earth Environmental Research, Nagoya University, Nagoya, Japan and <sup>6</sup>Botanical Gardens, Tohoku University, Sendai, Japan

**Corresponding authors:** Masaki Sano; Email: [fokienia@gmail.com](mailto:fokienia@gmail.com) and Masataka Hakozaiki; Email: [hakozaiki@rekihaku.ac.jp](mailto:hakozaiki@rekihaku.ac.jp)

**Received:** 20 December 2023; **Revised:** 26 March 2024; **Accepted:** 02 April 2024

**Keywords:** dendrochronology; oxygen isotopes; <sup>14</sup>C spike matching; Baitoushan volcanic eruption

## Abstract

We present an annual-resolution, millennium-long tree-ring chronology for northern Japan. The chronology is based on 5309 measurements of tree-ring  $\delta^{18}\text{O}$  from 37 samples of Hiba arbor-vitae (*Thujaopsis dolabrata* var. *honda*). Although the exact geographical origin of 27 of the samples is unknown because they were extracted from excavated archaeological material, pattern matching of the tree-ring  $\delta^{18}\text{O}$  variations was robust among all 37 samples. The floating chronology constructed using all samples was cross-dated against a previously published  $\delta^{18}\text{O}$  chronology from central Japan, yielding a correlation coefficient of 0.26 ( $t = 9.0$ ;  $p < 0.01$ ), resulting in a temporal coverage of 417–1595 CE (i.e., 1179 yrs). The global <sup>14</sup>C spike event at 774–775 CE was clearly recorded in the annual <sup>14</sup>C data, which provides independent support for the dating of tree rings using oxygen isotopes. Furthermore, this  $\delta^{18}\text{O}$  chronology from northern Japan was used to successfully cross-date a wood sample buried during the “Millennium Eruption” of Baitoushan, which is located on the border between China and North Korea.

## 1. Introduction

Oxygen isotope dendrochronology has developed rapidly in Japan over recent decades. The method is particularly useful because tree-ring  $\delta^{18}\text{O}$  levels are primarily governed by two climatic factors, the  $\delta^{18}\text{O}$  in precipitation and relative humidity (Ramesh et al 1986; Robertson et al 2001), both of which vary with the hydroclimate (i.e., wet–dry conditions) during the summer monsoon season in Japan (Nakatsuka et al 2020). Therefore, variations in tree-ring  $\delta^{18}\text{O}$  are closely correlated among different trees, irrespective of the species. Three millennial-scale  $\delta^{18}\text{O}$  chronologies have been produced for Japan, covering the past 4354 yrs (2349 BCE to 2005 CE). Two chronologies cover central Japan and the periods 612 BCE to 2005 CE (Nakatsuka et al 2020; Sano et al 2022) and 2349–1009 BCE, and the other covers northern Japan and the period 1412–466 BCE (Sano et al 2023). These chronologies have been widely used to date archaeological wood samples excavated in Japan (e.g., Sano et al 2022).

However, the available tree-ring  $\delta^{18}\text{O}$  dataset has spatial and temporal limitations. In particular, tree-ring  $\delta^{18}\text{O}$  data covering the last 2500 yrs—during which numerous radiocarbon age data have been derived from excavated wood—rely only on the single chronology from central Japan. Therefore, samples from sites distant from the origin of this chronology often cannot be dated. Spatial correlations of tree-ring  $\delta^{18}\text{O}$  series between any two samples distant from each other do not simply weaken



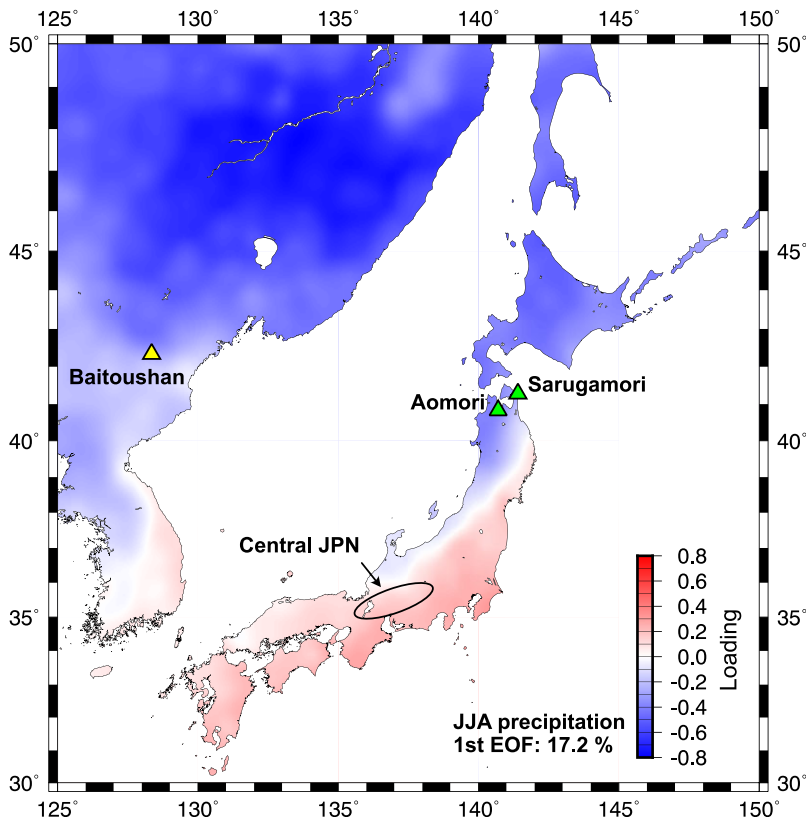


**Figure 1.** Map of Japan showing the locations of the Sarugamori and Aomori sites (green triangles), where dead trunk (Sarugamori) and archaeological (Aomori) samples were collected for this study; the Baitoushan site (yellow triangle), where sample C5 dated using the 774–775 CE radiocarbon spike event was collected (Hakozaki et al 2018a); and central Japan (oval), where 67 samples were collected for the 2617-yr master chronology that extends to the present day (Nakatsuka et al 2020; Sano et al 2022). Background colors represent first EOF loadings based on June–August precipitation data for the period 1891–2019 CE. We also used the Global Precipitation Climatology Centre (GPCC) Full Data Monthly Product Version 2020 (Schneider et al 2020) as our precipitation dataset ( $0.25^\circ \times 0.25^\circ$ ).

depending on their geographical distance, but are also modulated by the large-scale climatic conditions. The spatial pattern of summer precipitation is expressed as loadings of the first empirical orthogonal function (EOF; Figure 1). The signs (positive or negative) of the loadings, which represent correlations against the first EOF, split meridionally, highlighting the north–south contrast associated with the rainfall pattern across Japan. This pattern, which is enhanced by the Meiyu–Baiu front (a zonally oriented rain band), means that tree-ring  $\delta^{18}\text{O}$  series from two samples from a similar latitude (but distant from each other) will be relatively well-correlated. In fact, modern tree-ring  $\delta^{18}\text{O}$  data obtained from South Korea are closely correlated with our chronology from central Japan (Seo et al 2019), as both sites (ca. 1000 km apart) are located at a similar latitude. In contrast, two  $\delta^{18}\text{O}$  chronologies originating from different latitudes (ca. 400 km apart) in central and northern Japan show a significant but relatively weaker correlation (Sano et al 2023). These findings indicate that the development of a meridionally distributed tree-ring network is required if we wish to improve the performance of tree-ring dating in Japan, and possibly also across Korea and China.

High-resolution temporal records of radiocarbon content often allow us to determine the exact calendar year of a wood sample without using conventional tree-ring dating if a sharp spike in  $^{14}\text{C}$

concentration of precisely known age is present within a sequence of tree rings. Rapid changes in the  $^{14}\text{C}$  content of tree rings dated to 774–775 and 993–994 CE are good examples of this approach and have been observed in wood samples worldwide (Büntgen et al 2018; Miyake et al 2012; Park et al 2017). Such  $^{14}\text{C}$  spike events have been widely used for single-year radiocarbon dating (Hakozaki et al. 2018a, Kuitens et al 2022; Oppenheimer et al 2017; Meadows et al 2023; Philippsen et al 2022; Wacker et al 2014).

In this study, we developed a 1179-yr tree-ring  $\delta^{18}\text{O}$  chronology for northern Japan, using a total of 37 samples collected from two regions (Hakozaki et al 2011, 2016, 2017, 2018b). The chronology covers the period 417–1595 CE and was cross-dated against another  $\delta^{18}\text{O}$  chronology from central Japan (Nakatsuka et al 2020; Sano et al 2022). One of our cross-dated samples from the period 770–780 CE was also used for annual-resolution radiocarbon dating to verify our  $\delta^{18}\text{O}$ -based dates by reproducing the sharp  $^{14}\text{C}$  spike observed globally at 774–775 CE (Büntgen et al 2018). The utility of our newly developed chronology was evaluated by cross-dating a wood sample, which was buried by the “Millennium Eruption” of the Baitoushan volcano located on the border between China and North Korea. The tree-ring record from the master chronology is archived as Supplementary Material accompanying this article.

## 2. Materials and Methods

### 2.1. Study Sites and Sampling

The tree-ring samples used in this study were obtained from two regions in northern Japan (Figure 1). The first site was Sarugamori, where old, dead trunks of Hiba arbor-vitae (*Thujaopsis dolabrata* var. *hondae*) remain within a planted pine forest. These trees have been buried owing to the deposition of sand dunes, induced partly by past human activities (Okamoto et al 2000). A total of 10 samples were collected from trunks that were decaying in situ at Sarugamori. The second site was located in Aomori, which is ca. 80 km from Sarugamori. A total of 27 samples of Hiba arbor-vitae were collected from wooden material recovered from five archaeological sites, all of which were contained within a circle with a radius of ca. 15 km. As will be discussed later, the tree-ring  $\delta^{18}\text{O}$  series obtained from the samples from Sarugamori and Aomori are closely correlated, indicating that the geographical origin of these archaeological samples is not likely to have been far from Sarugamori. All 37 samples from the two regions were used to develop a master chronology for northern Japan. However, although we also measured the tree-ring widths of these samples, we were unable to successfully cross-date most of these series because they lacked common variations (see Supplementary Figure 1). We believe that the sampled trees had been growing at sites with little climate-related stress. Consequently, we excluded the ring-width series obtained from these samples from our study.

We also used one Korean pine sample (C5) from the Baitoushan (Changbaishan) volcano, which is located on the border between China and North Korea, to test the utility of tree-ring dating based on our master chronology. Tree rings from the C5 sample have been dated using the  $^{14}\text{C}$  spike at 774–775 CE (Hakozaki et al 2018a). The outermost ring of the sample with exterior bark was dated to 946 CE, which corresponds to the date of the “Millennium Eruption” (Oppenheimer et al 2017; Hakozaki et al 2018a). As the last 14 rings (933–946 CE) of the sample have been carbonized, the remaining inner part consisting of 298 rings (635–932 CE) was used for oxygen isotope analysis.

### 2.2. Tree-Ring Oxygen Isotope Data

Following the standard protocol for isotope dendrochronology (Kagawa et al 2015), cellulose was isolated directly from 1-mm thick wood plates while preserving the anatomical structures during chemical treatment. Each annual ring in the cellulose plates was manually separated from adjacent rings using a razor blade under a microscope. We loaded the annual ring samples (100–250  $\mu\text{g}$ ) into silver foil

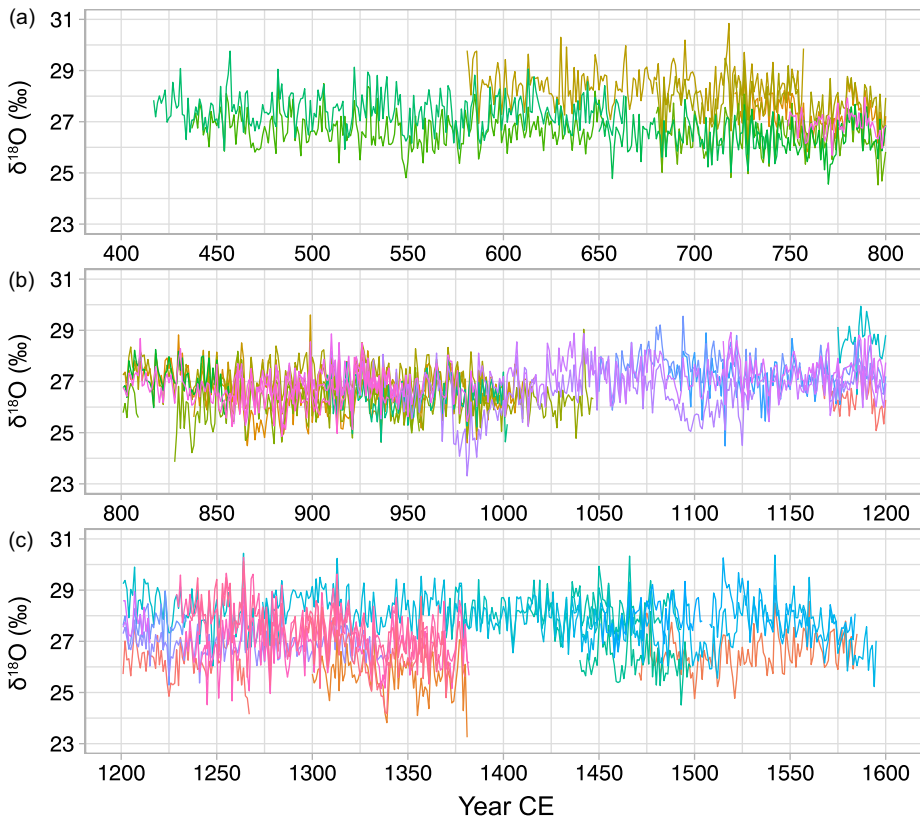


**Figure 2.** Plots of cross-dated raw tree-ring  $\delta^{18}\text{O}$  series from the Sarugamori and Aomori sites for the periods (a) 417–800, (b) 801–1200, and (c) 1201–1595 CE. The different colors of the plots designate the different  $\delta^{18}\text{O}$  series that were analyzed. Enlarged plots, together with sample legends, are presented in Supplementary Figure 2.

and then determined their oxygen isotopic compositions ( $^{18}\text{O}/^{16}\text{O}$ ) using a continuous flow mass spectrometer (Thermo Fisher Scientific Delta V Advantage) coupled to a pyrolysis-type elemental analyzer (Thermo Fisher Scientific High Temperature Conversion Elemental Analyzer). The oxygen isotope ratios are reported as  $\delta^{18}\text{O}$  (‰), with reference to the international Vienna Standard Mean Ocean Water (VSMOW). To reduce the analytical uncertainty, we used a nearly-zero-blank autosampler sealed against the atmosphere. Some 600 tree-ring samples were continuously measured in a single sequence that spanned 3 days. A laboratory standard material (Merck cellulose) was added every eight samples throughout the measurement procedure. The analytical uncertainty (i.e., 1 standard deviation) associated with the standard material was  $<0.20\text{‰}$ .

Pattern matching of the interannual  $\delta^{18}\text{O}$  variations was carried out to assign relative years to every ring of the 37 tree-ring series produced in this study. Correlation analysis was conducted using paired series to identify the relative years showing the highest correlation coefficients. However, the raw tree-ring  $\delta^{18}\text{O}$  series contain low-frequency variability (Figure 2), which may result in the inflation of correlation coefficients for incorrect dates. To avoid this, we used the high-pass filtered values of the tree-ring  $\delta^{18}\text{O}$  series for pattern matching. Relatively dated tree-ring  $\delta^{18}\text{O}$  series were then merged to form a chronology, which was used for pattern matching to identify the relative years of the remaining samples. This stepwise procedure of pattern matching was continued until every ring from all 37 series was relatively cross-dated.

A master chronology was developed by merging all 37 tree-ring  $\delta^{18}\text{O}$  series. The statistical properties of tree-ring  $\delta^{18}\text{O}$  differ from those of ring-width series. To account for this, Loader et al. (2019) proposed the use of a rectangular filter to standardize the raw tree-ring  $\delta^{18}\text{O}$  series. Specifically, a rectangular filter is easy to apply and enabled us to: 1) remove long-term trends; 2) minimize the loss of degrees of freedom; and 3) retain a low absolute autocorrelation (Loader et al 2019). Although we scrutinized rectangular filters ranging from 5 to 21 yrs in length, the choice of filter length was insensitive to the pattern matching, as was also found by Sano et al. (2022). To minimize autocorrelation and the loss of degrees of freedom, our master chronology was constructed using an 11-year rectangular filter, which is the same as previously applied to  $\delta^{18}\text{O}$  data from Japan (Sano et al 2022, 2023). Each of the raw tree-ring  $\delta^{18}\text{O}$  series was filtered and subtracted to produce anomalies with a mean of zero, and the resulting 37 series were then averaged to build the master chronology. The strength of the common variations in the standardized tree-ring  $\delta^{18}\text{O}$  series between different samples was evaluated using the mean inter-series correlation (Rbar) and the expressed population signal (EPS; Wigley et al 1984). Rbar is calculated by averaging the correlations derived from all pairs in a given time window, and the EPS indicates how well the chronology estimates a theoretically infinite population. The higher the sample size and/or Rbar, the closer the EPS approaches 1. An EPS value of 0.85 or more is a widely accepted threshold for the development of a robust chronology. We calculated the Rbar and EPS statistics using 50-yr windows, lagged by 25 yrs.

To assign the calendar years, we cross-dated our master chronology from northern Japan with a master chronology from central Japan (Figure 1; Nakatsuka et al 2020; Sano et al 2022). The latter was based on 67 samples consisting of Japanese cypress (mainly *Chamaecyparis obtuse*) and covers the past 2617 yrs (612 BCE to 2005 CE). Finally, a 298-yr tree-ring  $\delta^{18}\text{O}$  series from a Korean pine sample was compared with the two master chronologies from northern and central Japan to explore the utility of tree-ring oxygen isotope dating. The pattern-matching results were evaluated using a statistical test of correlation. Specifically, Student's *t*-test was applied using correlation coefficients and degrees of freedom that were corrected for autocorrelation and the statistical cost of the filter, so that they conformed to Student's *t* distribution (Loader et al 2019). The *t* values were converted into one-tailed probabilities (expressed conventionally as  $1/p$ ) that were corrected for multiple tests of significance using the Bonferroni correction (Dunn 1961). We applied the critical threshold of  $1/p \geq 100$ , proposed by Loader et al. (2019), to the results of the pattern matching. Our analysis was conducted using dplR (Bunn 2008, 2010) and other packages in the R environment (R Core Team 2020). The statistical data associated with the individual tree-ring  $\delta^{18}\text{O}$  series are provided in Supplementary Table 1.

### 2.3. Radiocarbon Measurements

To verify the tree-ring dates obtained via pattern matching of the oxygen isotope data, we conducted annual-resolution tree-ring  $^{14}\text{C}$  measurements for the period 770–780 CE, which covers the 774–775 CE radiocarbon spike event (Miyake et al 2012). Each of the 11 rings covering the period 770–780 CE from one of the Aomori samples (AONT001) was separated from its adjacent rings. Cellulose was extracted from small pieces of each annual ring using acid–alkali–acid and sodium chlorite treatments (Nakamura et al 2013). The graphite extraction and radiocarbon measurements were conducted at the Center for Chronological Research, Nagoya University (Nakamura et al 2007). We then compared our tree-ring  $^{14}\text{C}$  data with measurements from southern Japan (Miyake et al 2012) and from Baitoushan (Hakozaki et al 2018a).

## 3. Results and Discussion

The cross-dated raw and standardized tree-ring  $\delta^{18}\text{O}$  series from our 37 samples are shown in Figures 2 and 3, respectively (see Supplementary Figures 2 and 3 for enlarged plots with sample legends). Offsets from the mean  $\delta^{18}\text{O}$  values are evident among the samples, because our sampled trees were growing

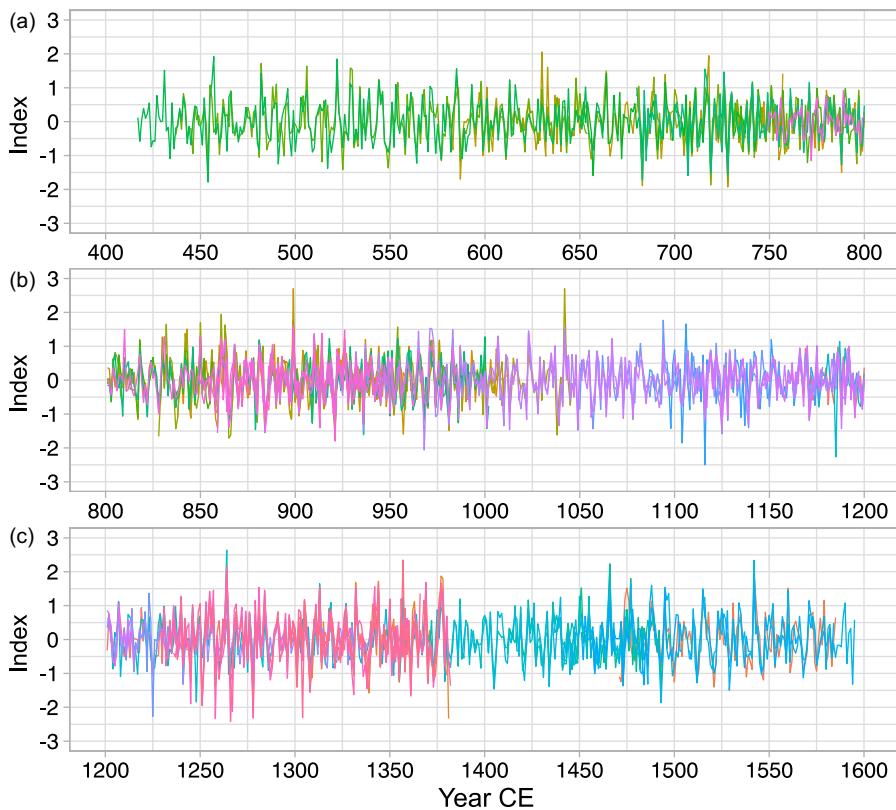


**Figure 3.** As for Figure 2, but for standardized tree-ring  $\delta^{18}\text{O}$  series. Standardization was conducted using an 11-yr rectangular filter to extract the high-frequency variability component. Enlarged plots, together with sample legends, are presented in Supplementary Figure 3.

over a wide region. Correlation matrices calculated using all pairs of overlapping periods of  $\geq 50$  yrs are presented in Supplementary Figures 4 and 5 for the raw and standardized series, respectively. Even though the mean  $\delta^{18}\text{O}$  values vary among the samples, all pairs of raw series show a statistically significant correlation ( $p < 0.05$ ), with a mean inter-series correlation coefficient of 0.58. We therefore consider the relative variations in annual  $\delta^{18}\text{O}$  to be well matched among the samples. Removing low-frequency variations using the 11-yr rectangular filter from the raw tree-ring  $\delta^{18}\text{O}$  series resulted in enhanced common variations among the samples (all pairs yielding  $p < 0.01$ ), with a mean inter-series correlation coefficient of 0.63. Our cross-dating was further tested using the leave-one-out principle. Specifically, standardized tree-ring  $\delta^{18}\text{O}$  series from one sample were correlated against a master chronology that was developed using the remaining samples. This showed that all 50-yr segments from any one sample are significant at  $p < 0.01$  (Supplementary Figure 6).

Overall, variations in tree-ring  $\delta^{18}\text{O}$  are closely correlated among the different samples, indicating the pattern matching is robust. The 1179-yr-long master chronology is presented in Figure 4, together with the number of samples and the Rbar and EPS values calculated using 50-yr windows. The Rbar values exceed 0.51 throughout the 1179 yrs, which statistically supports the reliability of our pattern matching. However, the EPS values (0.78–0.95) often do not attain the generally accepted threshold value of  $\geq 0.85$ , and this is largely because of the limited number of samples. Accordingly, a robust estimate of mean tree-ring  $\delta^{18}\text{O}$  is not achieved over the entire period of the chronology. On the other hand, as noted above, the pattern matching of our samples worked well; therefore, we consider the dating results to be reliable. In addition, our tree-ring dating based on this chronology is consistent with previously reported dendrochronological dates that are independent from our samples, as discussed below.



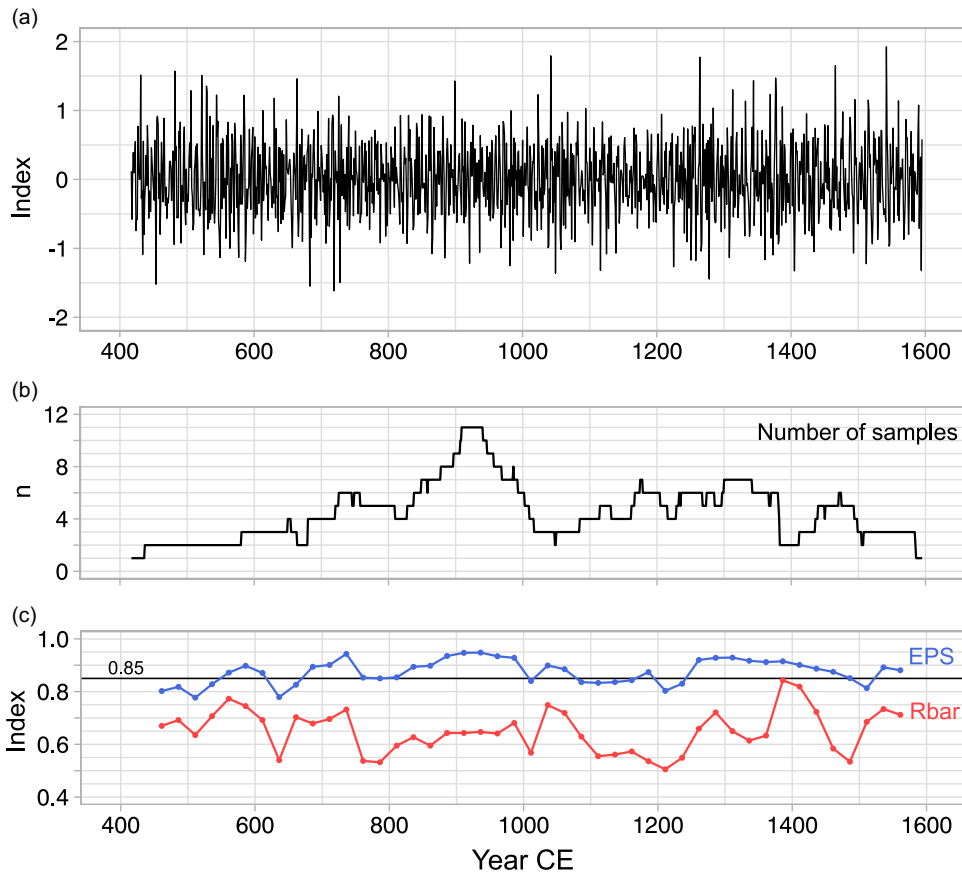


**Figure 4.** (a) The 1179-yr master chronology derived by averaging all standardized tree-ring  $\delta^{18}\text{O}$  series. An enlarged version of this plot is presented in Supplementary Figure 7. (b) Number of samples used for the master chronology. (c) Rbar and EPS statistics calculated for 50 yrs and lagged by 25 yrs.

The results of the pattern matching of our chronology against another chronology from central Japan (Nakatsuka et al 2020; Sano et al 2022) are presented in Figure 5. A high match in the  $t$  value of 9.0 ( $r = 0.26$ ,  $1/p > 10^6$ ) was observed when the last year of our chronology was placed at 1595 CE, which corresponds to the period 417–1595 CE. Remarkably high matches were also found using the early (417–1006 CE,  $t = 6.8$ ,  $r = 0.28$ ,  $1/p > 10^6$ ) and late (1007–1595 CE,  $t = 5.8$ ,  $r = 0.24$ ,  $1/p > 8 \times 10^4$ ) half-segments of our chronology. All of the pattern matching passes the critical threshold of  $1/p \geq 100$ , indicating that our tree-ring  $\delta^{18}\text{O}$  patterns were successfully cross-matched against the chronology from central Japan.

Our tree-ring chronologies from northern and central Japan for the common period 417–1597 CE are presented in Figure 6, together with sample sizes and running correlations. The running 51-yr correlations between the two chronologies show that the correlation tests alternated cyclically (period of 50–150 yrs) between significant and non-significant. As presented in Figure 1, the contrasting spatial distribution of hydroclimatic variability is seen with first EOF loadings based on June–August precipitation data for the period 1891–2019 CE. For the instrumental period, northern Japan (including our study region) is considered part of the Asian continental domain, whereas central Japan is part of the Japanese archipelago domain. Both master chronologies originate near the boundary between these two domains, and this boundary is likely to have shifted in the past in response to large-scale climatic conditions. This shifting of the boundary position seems to be at least partially responsible for the cyclical trends in periods showing significant or non-significant correlations between the two

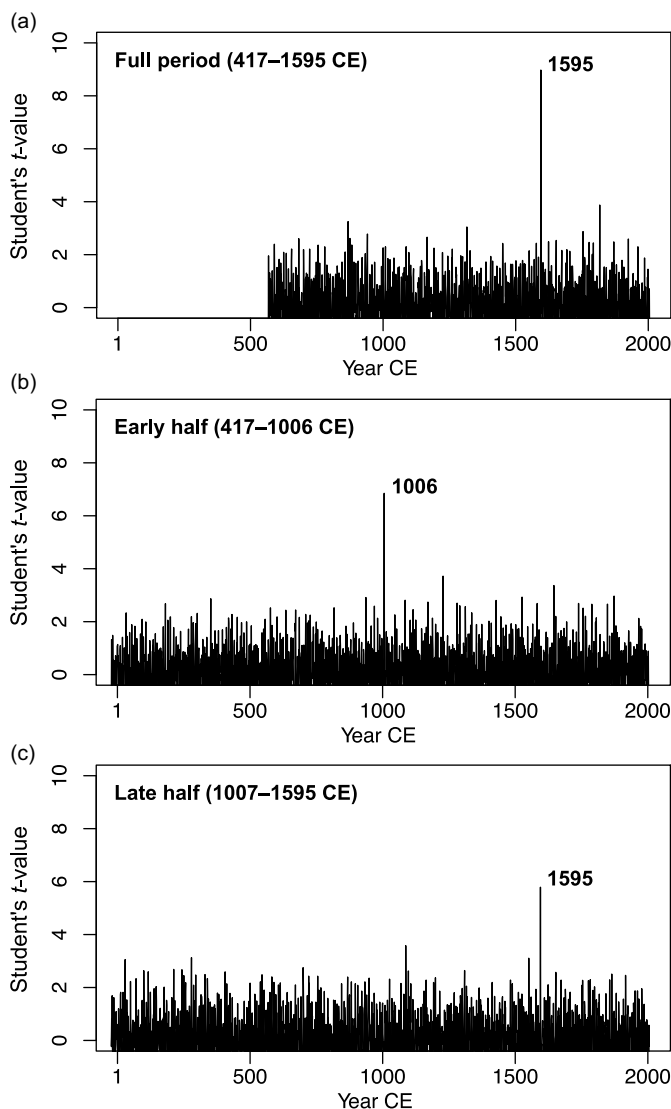


**Figure 5.** Distribution of Student's  $t$  values through time for all possible dates of our tree-ring  $\delta^{18}\text{O}$  chronology, using the periods (a) 417–1595, (b) 417–1006, and (c) 1007–1595 CE, against the master chronology from central Japan.

chronologies. We further scrutinized how the spatial correlations changed temporally during the instrumental period by analyzing the observed climate data from the Aomori weather station, which is located near our study sites, and also the ERA5 dataset (Hersbach et al 2020). Specifically, spatial correlations of precipitation and relative humidity for the June–August period from the ERA5 dataset were calculated against the corresponding Aomori station data for three periods (i.e., 1940–1967, 1968–1995, and 1996–2022 CE). Precipitation in Aomori was not significantly correlated with that in central Japan, but was correlated with that within a certain latitude range (ca.  $37^{\circ}$ – $45^{\circ}\text{N}$ ) for the three periods (Figure 7). Aomori precipitation shows a positive correlation with central Japan precipitation for the period 1968–1995 CE, although not statistically significant. Interestingly, this correlation was negative for the other two periods (1940–1967 and 1996–2022 CE). The shift in boundary position, as proposed above, is partially reproduced in terms of the spatial correlations of



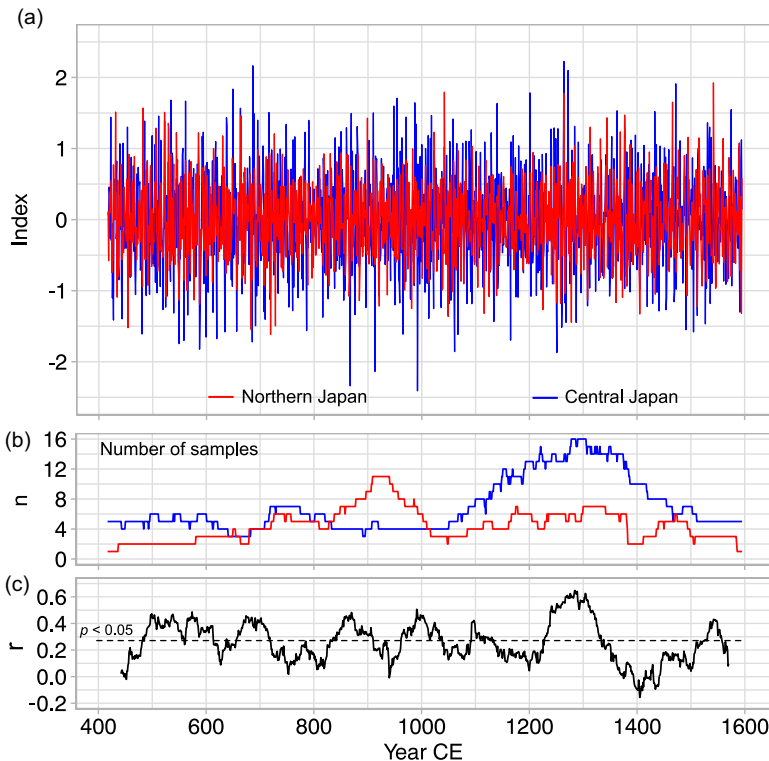


**Figure 6.** (a) Master chronologies for northern (this study) and central (Nakatsuka et al 2020; Sano et al 2022) Japan. An enlarged version of this plot is presented in Supplementary Figure 8. (b) Number of samples used for each master chronology. (c) Running 51-yr correlations between the two master chronologies.

precipitation. On the other hand, the correlations of relative humidity between Aomori and central Japan are much more temporally stable when compared with those for precipitation. Specifically, relative humidity in Aomori is significantly correlated with that in central Japan for the 1940–1967 and 1968–1995 CE periods. A temporal change in the spatial patterns of precipitation seems to be one of the main factors contributing to the unstable correlations between the two chronologies from northern and central Japan.

As shown in Figure 8, our annual-resolution radiocarbon record from northern Japan is closely correlated with that from southern Japan (Miyake et al 2012) and Baitoushan (Hakozaki et al 2018a). The sharp increase in  $^{14}\text{C}$  content observed globally at 774–775 CE (Büntgen et al 2018) is clearly reproduced in our measurements. Therefore, our tree-ring dates, derived from the pattern matching of oxygen isotope data, are independently verified by this  $^{14}\text{C}$  spike matching.

Our results of dating the Baitoushan sample against the master chronology from northern Japan are presented in Figure 9. The last year of the C5 sample was dated to 932 CE, which is consistent with the dating result derived independently from the  $^{14}\text{C}$  spike matching of the sample at 774–775 CE (Hakozaki et al 2018a). More specifically, the 298-yr series from Baitoushan is cross-dated against our master chronology from northern Japan for the period 635–932 CE, as clearly seen with a prominent peak in Student's  $t$  value of 6.45 ( $r = 0.37$ ; Figure 9). The probability ( $1/p$ ) of this pattern matching exceeds  $10^6$ , which passes the critical threshold of  $1/p \geq 100$ . However, pattern matching of this sample against the master chronology from central Japan failed, with no prominent  $t$  value observed over the past 2617 yrs. The  $t$  value was 0.97 at the correct date (932 CE), indicating that the master chronology from central Japan was unsuitable for dating sample C5 from Baitoushan. Figure 10 shows the running

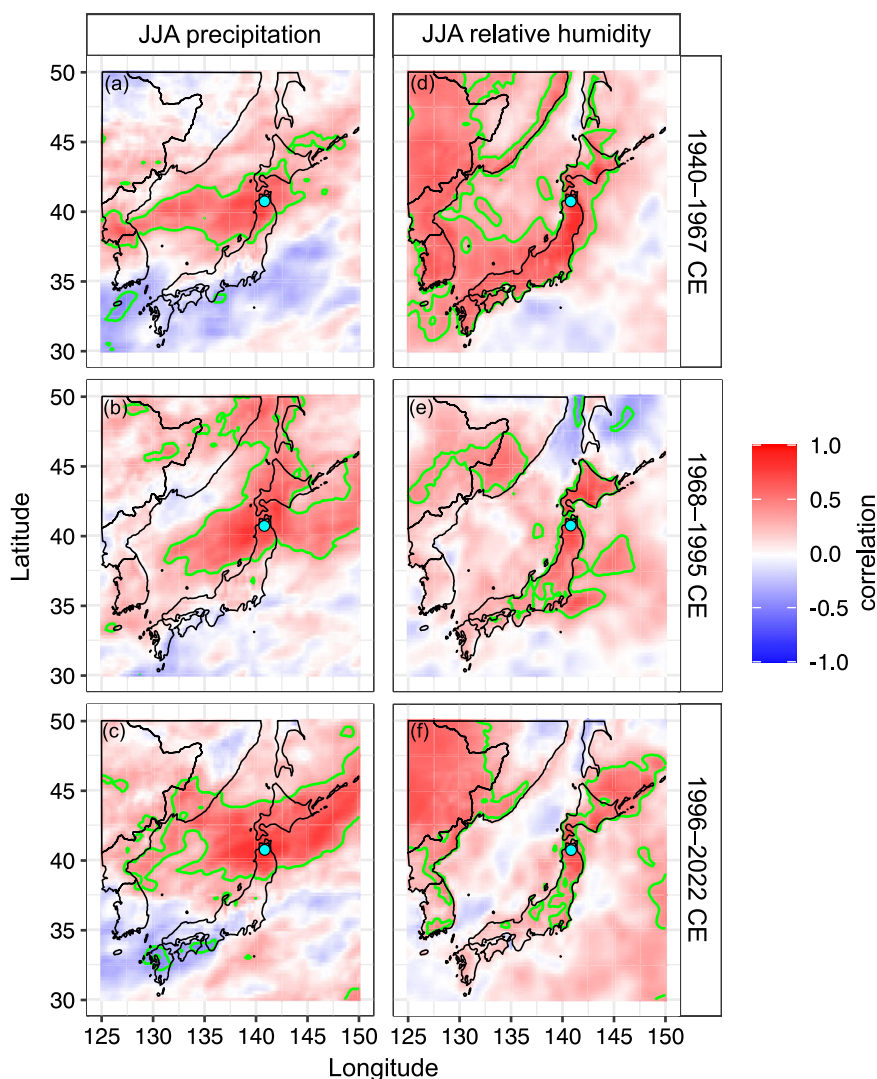


**Figure 7.** Spatial correlations between (a, b, c) precipitation and (d, e, f) relative humidity from the Aomori station (cyan circle) for the June–August period, and also data from the ERA5 dataset, for the periods (a, d) 1940–1967, (b, e) 1968–1995, and (c, f) 1996–2022 CE. Green lines enclose areas with significant correlations ( $p < 0.05$ ).

31-yr correlations for the Baitoushan  $\delta^{18}\text{O}$  series against the master chronologies from northern and central Japan. As the two chronologies are correlated (Figure 6), variations in their  $r$  values through time are similar (Figure 10b). Significant correlations are observed with the chronology from northern Japan, with non-significant correlations appearing in some periods, such as around 700, 750, and 880 CE. In contrast, the chronology from central Japan is less well correlated, with significant correlations appearing only in the period around 850 CE. These findings indicate that the northern Japan chronology exhibits certain advantages over the central Japan chronology for dating samples originating at higher latitudes on the Asian continent. Again, these contrasting results from tree-ring dating of the Baitoushan sample are related to the large-scale climatic controls on tree-ring  $\delta^{18}\text{O}$  levels. Our results highlight the importance of developing a spatially distributed tree-ring  $\delta^{18}\text{O}$  network over Japan, in particular for tree-ring data from different latitudes.

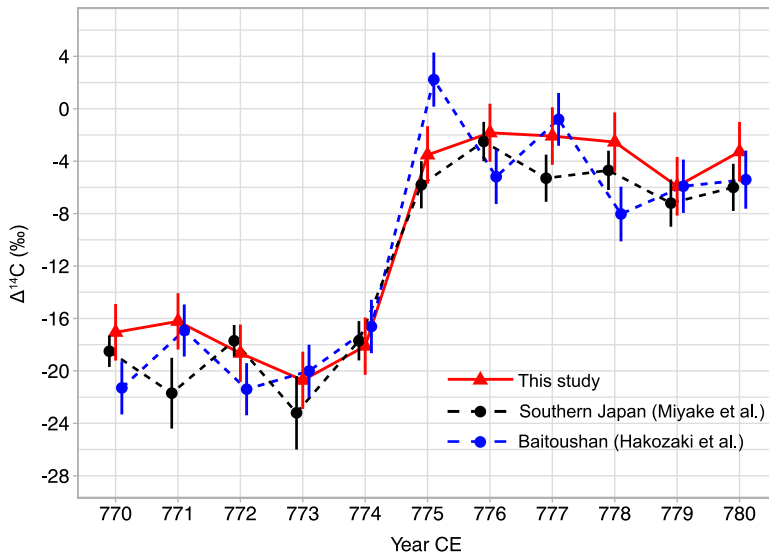


**Figure 8.** Comparison of annual-resolution tree-ring  $\Delta^{14}\text{C}$  time-series between our samples and those from southern Japan (Miyake et al 2012) and Baitoushan (Hakozaki et al 2018a).

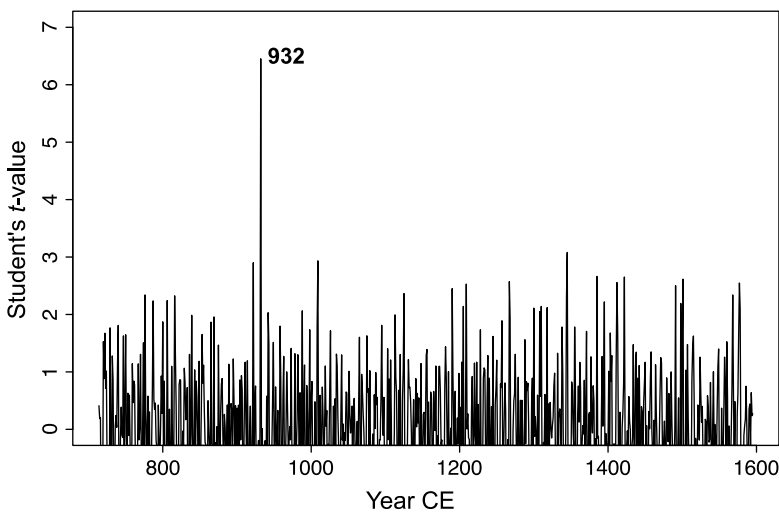


**Figure 9.** Distribution of Student's  $t$  values through time for all possible dates of the Baitoushan tree-ring  $\delta^{18}\text{O}$  series against the master chronology from northern Japan.

## Conclusions

We have developed a 1179-yr-long tree-ring  $\delta^{18}\text{O}$  chronology for northern Japan using 37 samples collected from dead trunks and unearthened wood from Hiba arbor-vitae. Our chronology was successfully cross-dated against another master chronology from central Japan. Our tree-ring dates were independently verified by reproducing the radiocarbon spike event at 774–775 CE. One sample from the Baitoushan site, which is located on the border between China and North Korea, was successfully cross-dated using our master chronology, clearly indicating the utility of tree-ring dating between samples from different countries. Continued efforts to develop tree-ring  $\delta^{18}\text{O}$  chronologies in and around Japan will contribute significantly to future tree-ring dating of wood samples.

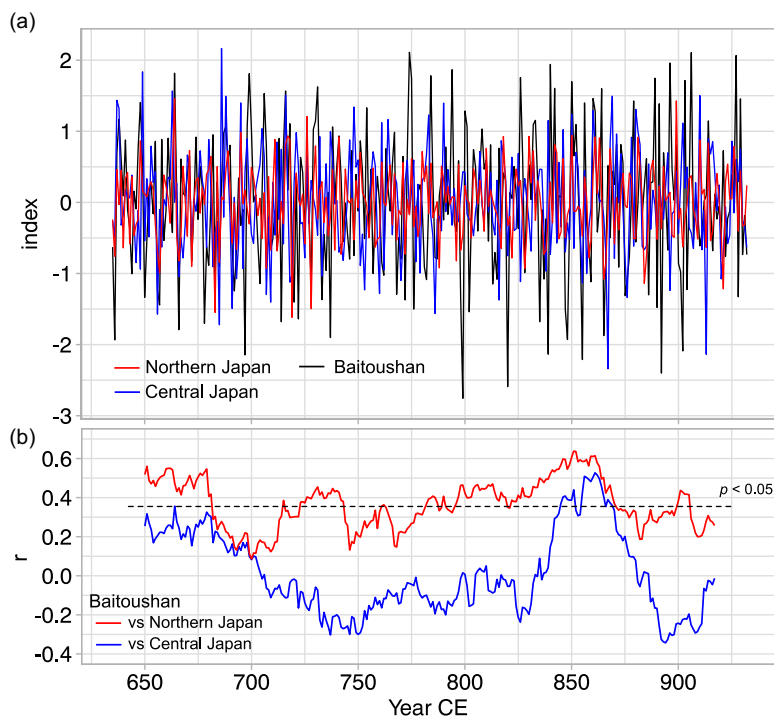


**Figure 10.** (a) Cross-dated tree-ring  $\delta^{18}\text{O}$  series from the Baitoushan site and the corresponding segment of the master chronologies from northern (this study) and central (Nakatsuka et al 2020; Sano et al 2022) Japan. (b) Running 31-yr correlations of the Baitoushan  $\delta^{18}\text{O}$  series against the master chronologies from northern and central Japan. Enlarged versions of these plots are presented in Supplementary Figure 9.

**Supplementary material.** To view supplementary material for this article, please visit <https://doi.org/10.1017/RDC.2024.55>

**Acknowledgments.** We are deeply indebted to the Boards of Education of Higashidōri Village and Aomori City, as well as the Aomori Prefectural Archaeological Artifacts Research Center, for granting permission to conduct our study. We thank Mitsuo Suzuki, Yasuharu Hoshino, Akihiro Yoshida, Takenori Yamamoto, Jun'ichi Kimura, and Hiromasa Nakasawa for their support in collecting tree-ring samples. This research was funded by the Research Institute for Humanity and Nature (Project 14200077) and Grants-in-Aid for Scientific Research from the Japan Society for the Promotion of Science (Grant nos 22500974, 22240082, 26750098, 26284120, 26244049, 17H04729, 17H06118, 20H00035, 22H00738, and 23H04845). We thank three anonymous reviewers and Associate Editor Steven Leavitt for their valuable comments, which helped to improve the manuscript.

**Declaration of Competing Interests.** The authors declare no conflicts of interest.

## References

- Bunn AG (2008) A dendrochronology program library in R (dplR). *Dendrochronologia* **26**, 115–124.
- Bunn AG (2010) Statistical and visual crossdating in R using the dplR library. *Dendrochronologia* **28**, 251–258.
- Büntgen U, Wacker L, Galván JD, Arnold S, Arseneault D, Baillie M, Beer J, Bernabei M, Bleicher N, Boswijk G, et al (2018) Tree rings reveal globally coherent signature of cosmogenic radiocarbon events in 774 and 993 CE. *Nature Communications* **9**, 3605.
- Dunn OJ (1961) Multiple comparisons among means. *Journal of the American Statistical Association* **56**, 52–64.
- Hakozaki M, Miyake F, Nakamura T, Kimura K, Masuda K and Okuno M (2018a) Verification of the annual dating of the 10th century Baitoushan volcano eruption based on an AD 774–775 radiocarbon spike. *Radiocarbon* **60**, 261–268.
- Hakozaki M, Nakamura T, Ohyama M, Kimura J, Sano M and Nakatsuka T (2016) Verification for the chronological age of woody remains from the Nitta (1) archaeological site in the Aomori city based on the AD774–775  $^{14}\text{C}$ -spike and  $\delta^{18}\text{O}$  dendrochronology. *Summaries of Researches Using AMS at Nagoya University* **27**, 34–39. In Japanese.
- Hakozaki M, Ohyama M, Hoshino Y and Sasaki Y (2011) Chronological relationships among the ruins inferred from tree-ring dating and radiocarbon dating of woody remains excavated from the Nitta No. 1 Site. *Report on Archaeological Research in Aomori City* **108**, 62–72. In Japanese.

- Hakozaki M, Sano M, Kimura K, Li Z, Tsushima A, Kobayashi K, Shidara S, Kimura J and Nakatsuka T (2017) Oxygen isotopic tree-ring dating of woody remains excavated from the Nakamichi and Kawaradate sites. *Report on Archaeological Research in Aomori City* **120**, 256–259. In Japanese.
- Hakozaki M, Sano M, Kimura K, Li Z, Tsushima A, Nakatsuka T, Kobayashi K and Nakasawa H (2018b) The oxygen isotopic tree-ring dating of the wood-parts of a well excavated from Yoneyama No. 2 site at Aomori City. *Bulletin of Aomori Prefectural Archaeological Artifacts Research Center* **23**, 1–12. In Japanese.
- Hersbach H, Bell B, Berrisford P, Hirahara S, Horányi A, Muñoz-Sabater J, Nicolas J, Peubey C, Radu R, Schepers D, et al (2020) The ERA5 global reanalysis. *Quarterly Journal of the Royal Meteorological Society* **146**, 1999–2049.
- Kagawa A, Sano M, Nakatsuka T, Ikeda T and Kubo S (2015) An optimized method for stable isotope analysis of tree rings by extracting cellulose directly from cross-sectional laths. *Chemical Geology* **393–394**, 16–25.
- Kuitens M, Wallace BL, Lindsay C, Scifo A, Doeve P, Jenkins K, Lindauer S, Erdil P, Ledger PM, Forbes V, Vermeeren C, Friedrich R and Dee MW (2022) Evidence for European presence in the Americas in AD 1021. *Nature* **601**, 388–391.
- Loader NJ, Mccarroll D, Miles D, Young GHF, Davies D and Ramsey CB (2019) Tree ring dating using oxygen isotopes: a master chronology for central England. *Journal of Quaternary Science* **34**, 475–490.
- Meadows J, Zunde M, Lēģere L, Dee MW, Hamann C (2023) Single-year <sup>14</sup>C dating of the lake-fortress at Āraiši, Latvia. *Radiocarbon*, 1–11. doi: [10.1017/RDC.2023.24](https://doi.org/10.1017/RDC.2023.24).
- Miyake F, Nagaya K, Masuda K and Nakamura T (2012) A signature of cosmic-ray increase in AD 774–775 from tree rings in Japan. *Nature* **486**, 240–242.
- Nakamura T, Masuda K, Miyake F, Nagaya K and Yoshimitsu T (2013) Radiocarbon ages of annual rings from Japanese wood: evident age offset based on IntCal09. *Radiocarbon* **55**, 763–770.
- Nakamura T, Miyahara H, Masuda K, Menjo H, Kuwana K, Kimura K, Okuno M, Minami M, Oda H, Rakowski A, Ohta T, Ikeda A and Niu E (2007) High precision <sup>14</sup>C measurements and wiggle-match dating of tree rings at Nagoya University. *Nuclear Instruments and Methods in Physics Research Section B: Beam Interactions with Materials and Atoms* **259**, 408–413.
- Nakatsuka T, Sano M, Li Z, Xu C, Tsushima A, Shigeoka Y, Sho K, Ohnishi K, Sakamoto M, Ozaki H, Higami N, Nakao N, Yokoyama M and Mitsutani T (2020) A 2600-year summer climate reconstruction in central Japan by integrating tree-ring stable oxygen and hydrogen isotopes. *Climate of the Past* **16**, 2153–2172.
- Okamoto T, Daimaru H, Ikeda S and Yoshinaga S (2000) Human impact on the formation of the buried forests of *Thuja* *dolabrata* var. *hondai* in the northeastern part of Shimokita Peninsula, northeastern Japan. *The Quaternary Research* **39**, 215–226. In Japanese with English abstract.
- Oppenheimer C, Wacker L, Xu J, Galván JD, Stoffel M, Guillet S, Corona C, Sigl M, Di Cosmo N, Hajdas I, Pan B, Breuker R, Schneider L, Esper J, Fei J, Hammond JOS and Büntgen U (2017) Multi-proxy dating the “Millennium Eruption” of Changbaishan to late 946 CE. *Quaternary Science Reviews* **158**, 164–171.
- Park J, Southon J, Fahrni S, Creasman PP and Mewaldt R (2017) Relationship between solar activity and  $\Delta^{14}\text{C}$  peaks in AD 775, AD 994, and 660 BC. *Radiocarbon* **59**, 1147–1156.
- Philippens B, Feveile C, Olsen J and Sindbæk SM (2022) Single-year radiocarbon dating anchors Viking Age trade cycles in time. *Nature* **601**, 392–396.
- R Core Team (2020) R: A language and environment for statistical computing: R Foundation for Statistical Computing, Vienna. URL <https://www.R-project.org/>.
- Ramesh R, Bhattacharya SK and Gopalan K (1986) Climatic correlations in the stable isotope records of silver fir (*Abies pindrow*) trees from Kashmir, India. *Earth and Planetary Science Letters* **79**, 66–74.
- Robertson I, Waterhouse JS, Barker AC, Carter AHC and Switsur VR (2001) Oxygen isotope ratios of oak in east England: implications for reconstructing the isotopic composition of precipitation. *Earth and Planetary Science Letters* **191**, 21–31.
- Sano M, Kimura K, Miyake F, Tokanai F and Nakatsuka T (2023) Two new millennium-long tree-ring oxygen isotope chronologies (2349–1009 BCE and 1412–466 BCE) from Japan. *Radiocarbon* **65**, 721–732.
- Sano M, Li Z, Murakami Y, Jinno M, Ura Y, Kaneda A and Nakatsuka T (2022) Tree ring oxygen isotope dating of wood recovered from a canal in the ancient capital of Japan. *Journal of Archaeological Science: Reports* **45**, 103626.
- Schneider U, Becker A, Finger P, Rustemeier E and Ziese M (2020) GPCP Full Data Monthly Product Version 2020 at 0.25°: Monthly Land-Surface Precipitation from Rain-Gauges built on GTS-based and Historical Data. DOI: [10.5676/DWD\\_GPCP/FD\\_M\\_V2020\\_025](https://doi.org/10.5676/DWD_GPCP/FD_M_V2020_025).
- Seo J-W, Sano M, Jeong H-M, Lee K-H, Park H-C, Nakatsuka T and Shin C-S (2019) Oxygen isotope ratios of subalpine conifers in Jirisan National Park, Korea and their dendroclimatic potential. *Dendrochronologia* **57**, 125626.
- Wacker L, Güttler D, Goll J, Hurni JP, Synal HA and Walti N (2014) Radiocarbon dating to a single year by means of rapid atmospheric <sup>14</sup>C changes. *Radiocarbon* **56**, 573–579.
- Wigley TML, Briffa KR and Jones PD (1984) On the average value of correlated time series, with applications in dendroclimatology and hydrometeorology. *Journal of Climate and Applied Meteorology* **23**, 201–213.

**Cite this article:** Sano M, Li Z, Tsushima A, Kimura K, Nakamura T, Ohyama M, Sakamoto M, Nakatsuka T, and Hakozaki M. A 1179-yr (417–1595 CE) tree-ring oxygen isotope chronology for northern Japan validated using the 774–775 CE radiocarbon spike. *Radiocarbon*. <https://doi.org/10.1017/RDC.2024.55>